Characterization of Surface Films Formed Prior to Bulk Reduction of Lithium in Rigorously Dried Propylene Carbonate Solutions

Seok-Gyun Chang, Hyo Joong Lee, Heon Kang, and Su-Moon Park*

Department of Chemistry and Center for Integrated Molecular Systems, Pohang University of Science & Technology, Pohang 790-784, Korea
Received January 12, 2001

Surface films formed prior to bulk reduction of lithium have been studied at gold, platinum, and copper electrodes in rigorously dried propylene carbonate solutions using electrochemical quartz crystal microbalance (EQCM) and secondary ion mass spectrometry experiments. The results indicate that the passive film formation takes place at a potential as positive as about 2.0 V *vs.* Li/Li^+, and the passive film thus formed in this potential region is thicker than a monolayer. Quantitative analysis of the EQCM results indicates that electrogenerated lithium reacts with solvent molecules to produce a passive film consisting of lithium carbonate and other compounds of larger molecular weights. The presence of lithium carbonate is verified by SIMS, whereas the lithium compounds of low molecular weights, including lithium hydroxide and oxide, are not detected. Further lithium reduction takes place underneath the passive film at potentials lower than 1.2 V with a voltammetric current peak at about 0.6 V.

Keywords : Surface films, Passivation, Lithium reduction, Propylene carbonate, Electrochemical quartz crystal microbalance, Secondary ion mass spectrometry.

Introduction

Electrochemical reduction of lithium ions in nonaqueous solutions has been studied extensively due to its importance in practical applications such as nonaqueous lithium rechargeable batteries.[1-14] While the stoichiometry of lithium reduction is simple, the reaction itself is rather complicated. The complications arise from a number of parameters including the dendritic growth of the lithium metal, its high reactivity, and complex electrode-electrolyte interfaces.[1] The lithium metal thus produced is more stable than the thermodynamics predicts in many solvents due to the formation of so-called solid-electrolyte interfaces.[15] Metallic lithium is also known to form an alloy with many metals.[16] When graphite electrodes are used, it is shown to be intercalated into the graphite lattices.[1-14,17-22] Before bulk reduction takes place at the thermodynamic potential, deposition of lithium compounds is observed at many electrodes due to the strong interaction of lithium with the electrode surface.[23] A number of studies have addressed this process.[23-29]

The underpotential deposition (UPD) of lithium on the electrode surface and its subsequent reactions were first studied by Li *et al.* employing far-infrared spectroelectrochemistry at the gold electrode in acetonitrile containing lithium perchlorate.[23] These investigators concluded that lithium thus formed was passivated by forming LiOH from its reaction with a small amount of water in the solvent. A similar result was reported by Xing *et al.* in propylene carbonate at a silver electrode.[24] Wagner and Gerischer concluded that LiH must be formed underneath the LiOH layer in acetonitrile containing water.[25,26] Later, Aurbach *et al.*[27-29] examined reduction of organic cations, as well as Li^+, in propylene carbonate and a few other organic solvents using electrochemical quartz crystal microbalance (EQCM) experiments, and concluded that trace amounts of dissolved oxygen are reduced forming LiO_2 at about 2.0 V, followed by reduction of water at about 1.3 V and lithium UPD at about 0.5 V.[29]

A better understanding of reactions of underpotentially deposited lithium with solvent molecules is very important in understanding passivation and degradation behaviors of lithium intercalated during the charging cycle of lithium batteries. Lithium intercalation,[30] another form of lithium UPD in graphite layers, is known to accompany co-intercalation of solvent molecules.[31] How the co-intercalated solvent molecules would react with underpoentially deposited lithium is very important in determining lithium battery performances.

Although efforts have been made to identify the chemical composition of the film, its composition is not fully identified. All the above investigators claim that water is responsible for the reaction after the lithium UPD. It is well established that the surface of lithium forms a passive film upon reaction with solvent molecules even in very rigorously dried solvents such as propylene carbonate.[15] This layer is called a solid-electrolyte interface (SEI) as the electron transfer takes place across it. In our present study, we address the deposition of lithium compounds in rigorously dried propylene carbonate in the underpotential region. A quantitative study was performed employing the EQCM experiments, and identification of the film was made by secondary ion mass spectrometry.

Experimental Section

Aldrich's anhydrous propylene carbonate (PC, 99.7% with

*Corresponding Author. e-mail: smpark@postech.edu

water contents < 0.005%) packaged under dried nitrogen in a sure seal™ bottle was purified by fractional distillation with a reflux ratio of 0.3 under reduced pressure of dried nitrogen after it was dried over activated molecular sieves for a few days. The distilled PC was then subjected to at least three freeze-pump-thaw cycles to remove dissolved air before it was moved to a glove box of an argon atmosphere. Southwestern Analytical's tetra-n-butylammonium perchlorate (TBAP, electrometric grade) and Aldrich's anhydrous $LiClO_4$ (99.99%), $LiPF_6$, $LiBF_4$, and $LiCF_3SO_3$ were dried overnight on a vacuum line.

Copper (Cu), gold (Au), and platinum (Pt) working electrodes were all homemade with their diameters of 1, 0.2, and 0.35 mm, respectively. The Au and Pt electrodes were sealed with soft glass and the Cu electrode was prepared by press-fitting into a Teflon rod. All electrodes were tested for leakage in KCl solutions containing potassium ferrocyanide or ferrocene by running repeated cyclic voltammetric experiments. A thin lithium piece cut from Aldrich's lithium foil (99.9%, packaged under argon gas) and a platinum foil were used as reference and counter electrodes, respectively.

All the experiments were carried out in a Vacuum Atmospheres model HE 493 glove box with the exception of EQCM measurements. Electrochemical measurements were made with an EG&G Princeton Applied Research model 273A or 283 potentiostat/galvanostat, which was controlled by an IBM PC compatible computer through an IEEE-488 bus controller card. An EG&G, Seiko model QCA917 quartz crystal microbalance was used to record the frequency shifts caused by the electrodeposition of lithium compounds and subsequent formation of passive films on the gold-coated quartz crystal electrode. Solutions prepared in an air tight cell in the glove box were used outside the glove box for EQCM measurements. During cyclic voltammetric scans, concurrent recordings of frequency shifts were made using the EQCM, and the experiments were controlled by the computer through an RS-232 serial port. A home built secondary ion mass spectrometer (SIMS) was used to analyze the chemical species of the film on the electrode. In SIMS experiments, samples were evacuated to 4×10^{-10} torr and the Cs^+ beam was used to sputter the analytes.

The working electrodes were polished with an alumina suspension (Buehler), finally with 0.05 μm with the exception of the carbon electrode before every experiment. The electrochemical cell was an H-type with two compartments separated by fritted glass. To remove impurities such as trace amounts of oxygen and water from the solution, preelectrolysis experiments were performed prior to main experiments in bulk scale in a cell containing a large platinum gauze electrode.

Results and Discussion

Cyclic voltammograms in the underpotential region. Figure 1 shows a cyclic voltammogram (CV) recorded at a gold electrode between 2.0 and -0.3 V *vs.* lithium in 1.0 M $LiClO_4$ at 10 mV/s. The CV shows bulk lithium reduction and its reoxidation. The lithium reduction starts well below 0.0 V, which suggests that some kind of a passive film might have been formed on the electrode surface. Although there seems to be only one pair of redox processes in Figure 1, a closer examination of the voltammogram recorded at a much higher sensitivity in the circled area shows that there are a number of current waves. These redox processes in this area are the main focus of this study.

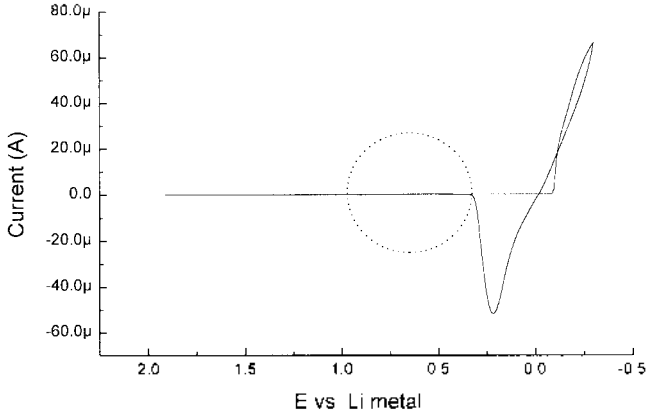

Figure 1. Cyclic voltammogram recorded at a gold electrode in 1.0 M $LiClO_4$ at10 mV/s.

Figure 2 shows a series of CVs recorded during four consecutive scans at the gold electrode between the open circuit potential (OCP, ~2.15 V) and 0.5 V, which display more detailed features than that shown in the circled area of Figure 1. The CVs are generally in agreement with those reported by Aurbach *et al.*[27-29] There are a few points to be noticed in this figure. First, the OCP shifts to negative values as the number of cyclic voltammetric scans. This suggests that electrogenerated lithium may form an alloy with the electrode and is not completely stripped off from the alloyed state. Second, at least three waves are observed prior to the bulk deposition of lithium as was the case in previous reports.[27-29] Third, no reversal currents are observed for the first two cathodic waves. Finally, the electrode is almost completely passivated with respect to the first wave but not the most cathodic wave.

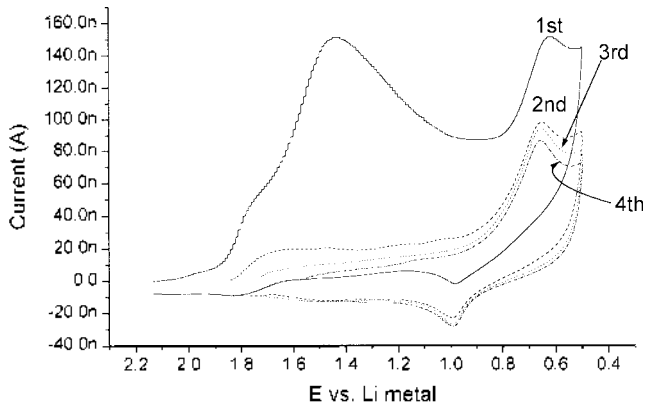

Figure 2. CVs recorded consecutively in 1.0 M $LiClO_4$ at the gold electrode at 10 mV/s. The scans started from open circuit potentials.

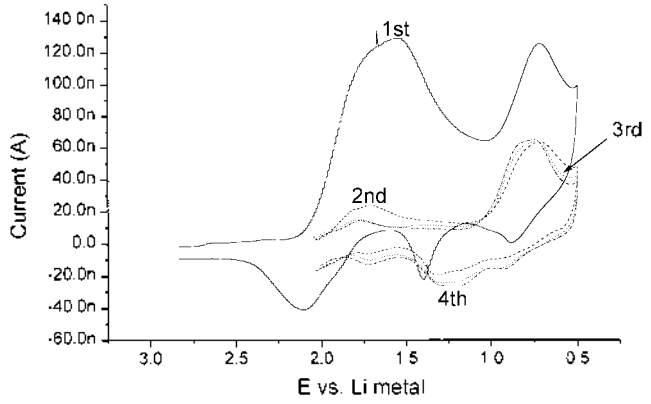

Figure 3. CVs recorded in 1.0 M $LiClO_4$ at a platinum electrode at 10 mV/s. The initial potential for each scan was the open circuit potential.

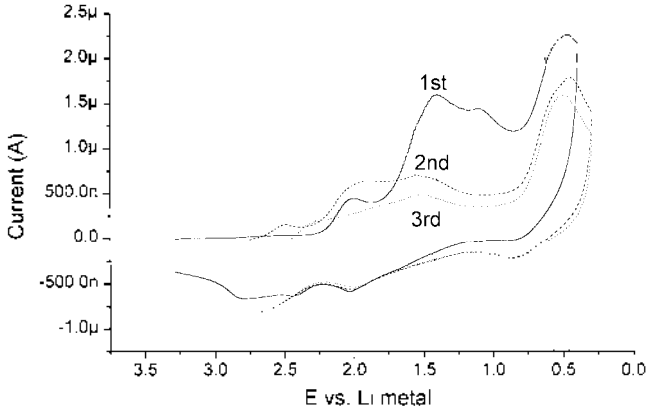

Figure 4. CVs recorded in 1.0 M $LiClO_4$ at a copper electrode at 10 mV/s. The initial potential was the open circuit potential.

Similar results were obtained from other electrodes, although minor details were different. CVs recorded at Pt and Cu electrodes in 1.0 M $LiClO_4$ solutions are displayed in Figures 3 and 4. When other electrolyte salts such as $LiPF_6$, $LiBF_4$, and $LiCF_3SO_3$ were used, basically similar results were obtained.

Figure 5 shows a comparison of the first CVs obtained at these electrodes and a CV recorded at the gold electrode in the absence of Li^+ (Figure 5d). These CVs were obtained at fresh electrodes during the first scans. As the platinum electrode has the best electrocatalytic activity for water reduction among electrodes tested here,[32] it is expected to show the lowest overpotential and the highest CV current if water is responsible for these prewaves. In other words, if the water reduction affected the degree of the passive film formation as were previously reported,[23-29] it would have been most severe at the platinum electrode under given experimental conditions. Our results show that the gold electrode shows the highest current flowing during the first CV scan.

As a final point, we ran experiments in which the trace amount of water was removed from the electrolyte solution by preelectrolysis at 0.70 V with a large platinum gauze electrode, while the solution is vigorously stirred, until the current falls to 0. The CVs recorded at the small indicator working electrode after the preelectrolysis were identical to the ones recorded before the removal of water. When water was removed from the solution by adding pieces of lithium metal with the solution stirred for about two hours, we obtained the same CV results. These experimental results suggest that it is *not* water that causes the prewaves observed starting at about 2 V.

Electrochemical quartz crystal microbalance measurements. To see if the lithium deposition at potentials more positive than 0.0 V follows Faraday's law, EQCM experiments were performed at a gold coated quartz crystal electrode. Figure 6 shows frequency shift data recorded at a gold-coated quartz crystal electrode as a function of scanning potential in 1.0 M $LiClO_4$. Control experiments run with 1.0 M TBAP as an electrolyte in the same potential range as in Figure 6 gave almost no frequency changes. From the result shown here, we can see that the passive films are formed upon deposition of lithium as the frequency keeps decreasing even during the anodic scan. If the deposited lithium is anodically stripped, the frequency would have resumed its initial value. The change in weight, Δm, was calculated from the change in frequency, Δf, using the Sauerbrey equation.[33]

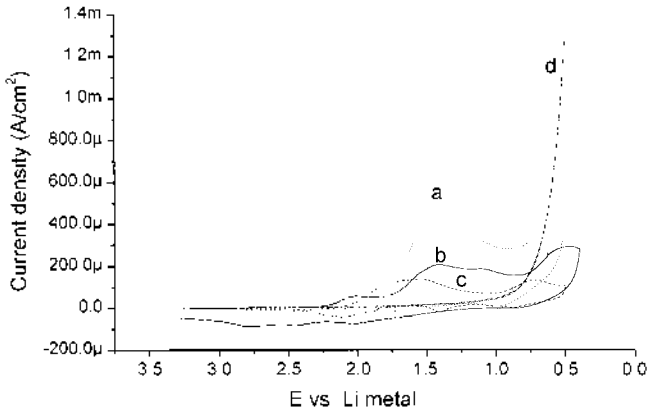

Figure 5. CVs recorded at: (a) gold, (b) copper, and (c) platinum electrodes in 1.0 M $LiClO_4$, and (d) gold electrode in 0.2 M TBAP. The sweep rate was 10 mV/s.

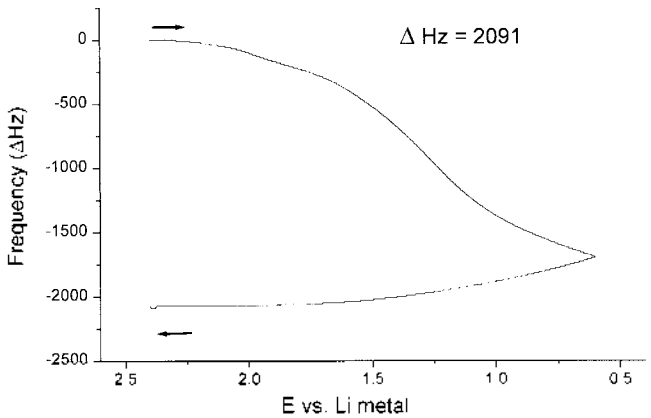

Figure 6. The frequency shift *vs.* potential plot recorded at 10 mV/s for the first potential cycle.

Table 1. Weight Increase Observed at a Gold Electrode upon Potential Scanning

	1st scan	2nd scan	3rd scan	4th scan
Scan range (V)	2.4 → 0.6 → 2.4	2.4 → 0.5 → 2.4	2.4 → 0.5 → 2.4	2.4 → 0.5 → 2.4
$\Delta w_{Li,calc}$[a], μg/cm²	0.99	0.34	0.21	0.22
$\Delta w_{forward}$[b], μg/cm²	6.02	0.26	0.19	0.16
$\Delta w_{reverse}$[c], μg/cm²	1.38	0.30	0.18	0.14
Δw_{total}[d], μg/cm²	7.40	0.56	0.37	0.30
$\Delta M_{total}/\Delta M_{calulated}$	7.5	1.6	1.7	1.4

[a]$\Delta w_{Li,calc}$ is the amount of lithium deposited calculated from the charge passed. [b]$\Delta w_{forward}$ is the weight increase observed during the forward potential scan. [c]$\Delta w_{reversal}$, the weight change observed during the reversal scan; and [d]Δw_{total} is the total weight change observed during the full scan ($=\Delta w_{forward} - w_{reversal}$).

$$\Delta m = -C_f \cdot \Delta f,$$

assuming that the weight change is a major contribution to the change in frequency.[29] Here C_f is a proportionality constant related to the physical properties of the quartz crystal as well as solvent properties. From the calibration experiment using electrodeposition of silver under an identical condition, this constant was found to be 11 ng Hz^{-1} cm^{-2}.

Results obtained for four consecutive potential scans are summarized in Table 1. Again, there are a few points that are noticed from this result. First, the major fraction of lithium deposition takes place during the first scan. From the second scan on, not much weight increase is observed. Second, no anodic stripping is observed from the electrodeposited lithium, although a small amount of anodic current flows upon potential reversal (Fig. 2). This means that electrodeposited lithium immediately undergoes oxidation *via* chemical reactions and is primarily in the +1 state. The anodic current may result from stripping of a small amount of lithium alloyed into the electrode. Third, the amount of the deposit (Δw_{total}) on the electrode surface is much larger than the one calculated from the cathodic charge passed ($\Delta w_{Li,calc.}$) during the scan, had the deposit been only metallic lithium. This indicates that the deposit is not metallic lithium but its compounds immediately formed upon electrodeposition. The actual increase in weight is much larger than the one that would have been obtained if lithium had been converted to variously hydrated hydroxides, superoxide, or even lithium carbonate, as postulated by Aurbach *et al.*[28] The ratio of the total deposited weight to that theoretically calculated is as large as 7.5 during the first cycle, going down to about 1.4 in the fourth cycle (Table 1). When Li_2CO_3, LiO_2, Li_2O, or LiOH are produced as was postulated by Aurbach *et al.*,[27-29] their expected ratios would be 5.3, 5.6, 3.3, and 3.4, respectively. Thus, the film must contain significant fractions of compounds of larger molecular weights than any of these compounds. In other words, our results suggest that the reaction products formed between electrogenerated lithium and the solvent molecules *must be* present in the passive film.

The reaction of PC with electrogenerated lithium to form lithium carbonate has been well documented in the literature;[3,12,14,34,35] however, lithium carbonate alone does not explain the high ratio of about 7.5 for the observed weight increase to that theoretically calculated from the charge. Again, this means that a lithium compound with a larger molecular weight than lithium carbonate must also have been formed. One possibility is the reduction of the carbonyl group on PC molecules by electrogenerated lithium to the corresponding alcohol whose proton is replaced by the lithium ion. Thus, the major fraction would be lithium carbonate with a minor fraction of a larger molecular weight than the carbonate. Aurbach *et al.* identified alkylcarbonates as the main components in their study of surface films formed upon lithium reduction in PC.[36]

Fourth, the amount of the deposit becomes much smaller after the first scan. Here the ratio of the weight change observed to that calculated is not as large as for the first scan (~1.4 *vs.* 7.5) as pointed out above. This is probably because lithium formed underneath the passive layer at the most cathodic wave is protected from the solvent molecules and only a minor fraction thus formed undergoes reactions with them.

In conclusion from the observations described thus far, the mechanisms proposed by previous investigators[23-29] do not fully explain our observations during the lithium deposition in the underpotential region. The film deposited during the first scan has too high mass accumulated per electron discharged if they were lithium superoxide, oxide, and/or hydroxide, which would have resulted from electrolysis of oxygen or water.

In an ideal situation where the faradaic current is accompanied by the weight increase with 100% of coulombic efficiency, the derivative signal corresponding to the rate of weight increase upon electrolysis should have an identical shape to that of the CV.[37] We thus obtained derivative signals from frequency shifts by numerical differentiation and the result for the first potential scan is shown in Figure 7(a). As we can see, the $d\Delta f/dt$ signal has significantly different features from those of the first CV shown in Figure 2, indicating that the mechanism for lithium deposition is complex. Also, in no case is there a decrease in weight during the anodic electrochemical scan. Three reasonably resolved peaks, which correspond roughly to the potentials for the CV peaks shown in Figure 2 except for the most negative one at about 0.6 V, are observed. No maximum rate of deposition is observed at about 0.6 V in Figure 7a where the lithium UPD is supposed to take place,[28] although the maximum current is observed in the CV. This is probably because the lithium deposition taking place underneath the passive film at this potential represents relatively a minor fraction of the weight increase compared to that from the chemical reaction of lithium with solvent molecules. In other words, the weight increase due to the lithium deposition at this potential must be relatively small compared to that due to the chemical reaction of lithium. When the current is low as in the case of the second scan, the maximum rate of deposition appears at about 0.6 V as can be seen in Figure 7(b). From the second scan on, the rate of weight increase is positive below about

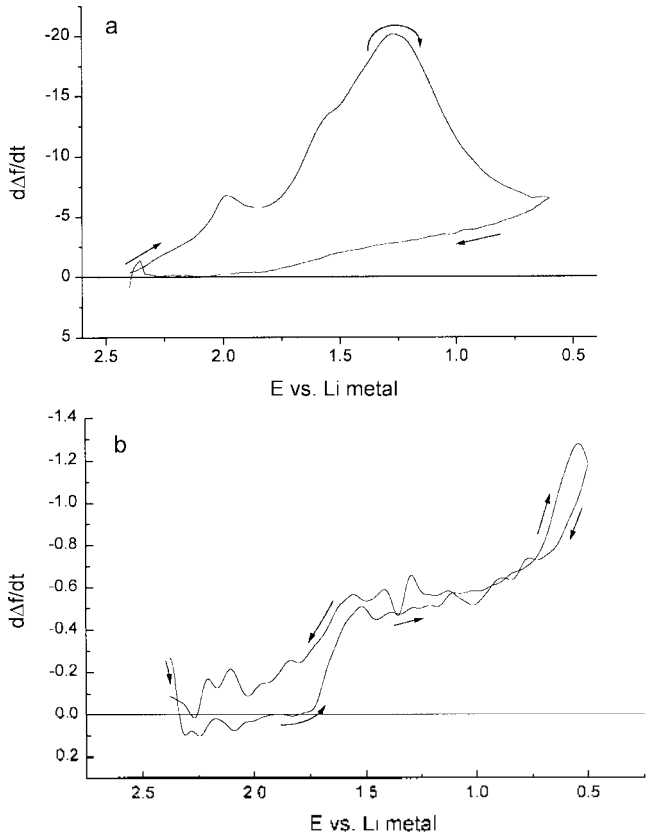

Figure 7. The dΔf/dt *vs.* potential plot obtained from the data for the first cycle shown in Figure 6 (a); and the dΔf/dt *vs.* potential plot obtained for the second cycle (b).

1.75 V indicating that the weight increase is observed even during the reversal scan also. The same pattern of the weight increase is observed after the second scan.

Secondary ion mass spectroscopy. In order to identify the chemical species of the film, we ran secondary ion mass spectrometry (SIMS) experiments. After samples were subjected to vacuum of lower than 4×10^{-10} torr. Cs^+ ion beams were used to sputter the surface species of the passive films formed on the electrode, and a quadruple mass spectrometer was used to detect the cations ejected from the surface. The samples were obtained by running repeated potential scans in 1.0 M $LiClO_4$. Two types of samples were prepared depending on the scan range. One was obtained by scanning potentials repeatedly between 2.4 and 1.2 V, which corresponds to the more positive prewave peaks; another was between 2.4 and 0.5 V, which includes the most negative UPD peak. After the potential scans, the samples were washed several times with PC and then dried in a vacuum line at about 4×10^{-5} torr for two days. When the samples were placed inside the SIMS chamber, a considerable pressure increase was observed from 4×10^{-10} to 4×10^{-8} torr, although they had been dried for over two days under vacuum. The SIMS measurements were then made after the vacuum was stabilized at 4×10^{-10} torr for some period.

Figures 8 and 9 show the SIMS spectra obtained from the films. Note that the energy of a primary Cs^- beam was 30-

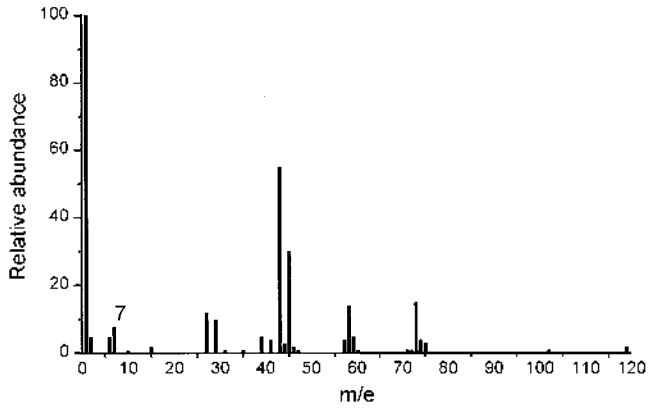

Figure 8. The mass spectrum of the film formed on the gold electrode. The potential scan range was between 2.4 V and 1.2 V at an Au electrode, the number of the voltage scan was 6, the energy of the incident Cs^+ ion beam was 30 eV, and the number of SIMS scan was 23.

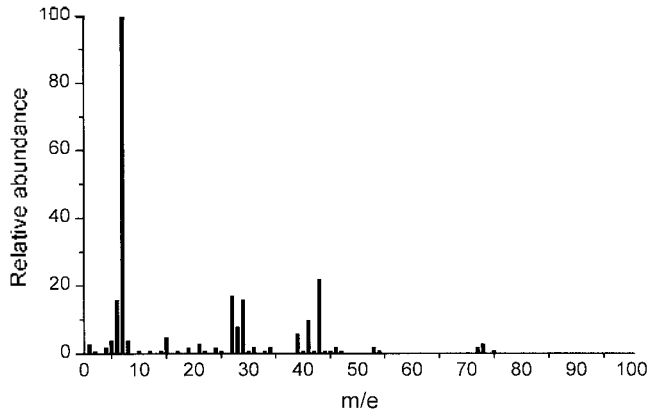

Figure 9. The mass spectrum of the film formed on the gold electrode. The eight voltage scans were made between 2.4 and 0.5 V and the number of SIMS scans was 10 with the Cs^- beam energy of 100 eV.

100 eV, much lower than in conventional SIMS experiments that employ keV beams. This low energy mode has a few unique advantages over the keV experiments.[38] First, fragmentation of molecular species is much reduced, because the incident beam energy is barely above the desorption threshold of molecular ions.[39] Second, only the species on the top-layer are ejected and detected by the beam collision. This allows analysis of the species contained only in the outer layer. These features are well reflected in the spectra shown in Figures 8 and 9, the mass assignment of the detected ions being summarized in Table 2. The spectra show large populations for high molecular weight species in addition to atomic ions. The peaks at 58 and 74 amu are assigned to $Li_2CO_2^+$, and $Li_2CO_3^-$, respectively, verifying the large abundance of Li_2CO_3 in the passive layer asserted from the EQCM study. If the lithium-PC adduct were present, the PC ion and many forms of its decomposition fragments may also be present. The PC parent peak is indeed detected, though low in its intensity, because of its very low ionization efficiency compared with other metal containing compounds

Table 2. Detected Masses of Ions and Their Assignments

Mass	Possible ions	Mass	Possible ions
1	H^+	41	K^-, $C_3H_5^+$
6, 7	Li^-	43	AlO^-, $C_3H_7^+$
15	CH_3^-, Li_2H^-	45	$Li_2CH_3O^+$
27	Al^-	56-58	$Li_2CO_2^-$
29	$C_2H_5^+$	72-74	$Li_2CO_3^-$
39	K^+	102	PC^+

appearing in the spectra. Significantly, $LiOH^+$ (24 amu) and Li_2O^+ (30 amu) are not observed. supporting the EQCM analysis that their concentrations should be very low even if they are present. There appear a few additional peaks that can be assigned to either alkyl cations [CH_3^+ (15 amu). $C_2H_5^-$ (29 amu), $C_3H_5^+$ (41 amu). and $C_3H_7^+$ (43 amu)] originating from PC or metallic impurities such as Al^- (27 amu). AlO^+ (43 amu), and K^+ (39 and 41 amu). These metal impurity ions must have come from alumina slurries introduced while polishing the electrode surfaces. According to Aurbach and Gottlieb,[27] only LiO_2 and/or hydrated LiOH would have been produced in the potential range of 2.4-1.2 V. However. it is seen from Figure 8 that Li_2CO_3 and even PC peaks are detected from the film obtained in this potential region. This indicates that the passive film resulted not from the reduction products of oxygen and/or water.

The SIMS spectrum shown in Figure 8 was obtained using a 30 eV Cs^+ beam. When the ion beam energy was increased to 100 eV (not shown). essentially the same spectral pattern was obtained except that the relative intensity for the Li^+ increased significantly, while other signals stayed approximately the same. The higher energy Cs^- beam caused more severe fragmentation of the Li-containing molecular species. increasing the Li^- signal intensity in the spectrum. Considering that the signal for atomic Li^+ is weaker than those for $Li_2CO_2^+$ and $Li_2CO_3^+$ for the 30 eV beam (Figure 8), and that the atomic Li^- ejection can arise from collisional decomposition of the carbonate as well as from Li in its bulk metallic state. we conclude that the portion of metallic Li is relatively minor in the deposited film. In Figure 9. the intensity for Li^+ is stronger than high molecular weight ions as the incidence beam energy is increased to 100 eV. For this reason. the peak for PC is not observed.

Conclusion

We have investigated the underpotential deposition of lithium from lithium perchlorate solutions at gold, platinum. and copper electrodes in *rigorously dried* PC solutions using various techniques including cyclic voltammetry. EQCM. and SIMS experiments. The CV results indicate that underpotentially deposited lithium undergoes a chemical reaction and passivates the surface. The EQCM results confirm this being the case and allows us to deduce the composition of passive films. From excessive increases in weight observed during the first potential scan, we conclude that the major fraction of the passive film formed on the surface must be lithium carbonate along with some other high molecular weight compounds such as alkyl carbonates. Detection of alkyl groups in SIMS spectra also is consistent with the presence of alkylcarbonates. Lithium hydride. lithium hydroxide, and lithium superoxide may be produced during the second and third scans underneath the passive layer, but not significantly during the first scan. The low energy SIMS experiment provides direct evidence for the lack of these compounds. The passive layer on the surface contains mostly lithium carbonate and other high molecular weight compounds including alkylcarbonates, but lithium oxide. hydroxide and lithium superoxide exist in negligible amounts if they do.

In conclusion, the reaction between the underpotentially deposited lithium and solvent molecules in solution produces a passive film. The passive film does not result from reduction of trace amounts of oxygen and/or water in *rigorously* dried solvents. The high reactivity of lithium must shift the equilibrium of the system. resulting in a large shift in its reduction potential in a positive direction. The difference between our and previously reported observations must have resulted from the amount of water and dissolved oxygen present in solutions. Experimental results obtained before and after the preelectrolysis with a large platinum electrode support this conclusion also.

Acknowledgment. A grateful acknowledgement is made to Korea Science & Engineering Foundation for supporting this work through the Center for Integrated Molecular Systems. Graduate stipends were provided by the Korea Research Foundation through its BK21 program.

References

1. Scrosati, B. *J. Electrochem. Soc.* **1992**, *139*, 2776.
2. Fischer, J. E.; Thompson, T. E. *Phys. Today* **1978**, *31*, 36.
3. Aurbach, D.; Ein-Eli, Y. *J. Electrochem. Soc.* **1995**, *142*, 1746.
4. Tatsumi, K.; Iwashita, N.; Sakaebe, H.; Shioyama, H.; Higuchi, S. *J. Electrochem. Soc.* **1995**, *142*, 716.
5. Dahn, J. R. *Phys. Rev. B* **1991**, *44*, 9170.
6. Ohzuku, T.; Iwakoshi, Y.; Sawai, K. *J. Electrochem. Soc.* **1993**, *140*, 2490.
7. Yazami, R.; Touzain, Ph. *J. Power Sources* **1983**, *9*, 365.
8. Takami, N.; Satoh, A.; Hara, M.; Ohsaki, T. *J. Electrochem. Soc.* **1995**, *142*, 371.
9. Dahn, J. R.; Fong, R.; Spoon, M. J. *Phys. Rev. B* **1990**, *42*, 6424.
10. Jiang, Z.; Alamgir, M.; Abraham, K. M. *J. Electrochem. Soc.* **1995**, *142*, 333.
11. Morita, M.; Hayashida, H.; Matsuda, Y. *J. Electrochem. Soc.* **1987**, *134*, 2107.
12. Shu, Z. X.; McMillan, R. S.; Murray, J. J. *J. Electrochem. Soc.* **1993**, *140*, 922.
13. Fong, R.; Von Sacken, U.; Dahn, J. R. *J. Electrochem. Soc.* **1990**, *137*, 2009.
14. Dey, A. N.; Sullivan, B. P. *J. Electrochem. Soc.* **1970**, *117*, 222.
15. Peled, E. *J. Electrochem. Soc.* **1979**, *126*, 2047.
16. Dey, A. N. *J. Electrochem. Soc.* **1971**, *118*, 1547.

17. Farcy, J.; Messina, R.; Perichon, J. *J. Electrochem. Soc.* **1990**, *137*, 1337.
18. Kumagai, N.; Matsuura, Y.; Tanno, K. *J. Electrochem. Soc.* **1992**, *139*, 3553.
19. Kumagai, N.; Fujiwara, T.; Tanno, K. *J. Electrochem. Soc.* **1993**, *140*, 3194.
20. Kanehori, K.; Kirino, F.; Kudo, T.; Miyauchi, K. *J. Electrochem. Soc.* **1991**, *138*, 2216.
21. Guyomard, D.; Tarascon, J. M. *J. Electrochem. Soc.* **1992**, *139*, 937.
22. Baranski, A. S.; Fawcett, W. R. *J. Electrochem. Soc.* **1982**, *129*, 901.
23. Li, J.; Pons, S.; Smith, J. J. *Langmuir* **1986**, *2*, 297.
24. Xing, X. K.; Abel, P.; McLintyre, R.; Scherson, D. *J. Electroanal. Chem.* **1987**, *216*, 261.
25. Gerischer, H.; Wagner, D. *Ber. Bunsenges. Phys. Chem.* **1988**, *92*, 1325.
26. Wagner, D.; Gerischer, H. *Electrochim. Acta* **1989**, *34*, 1351.
27. Aurbach, D.; Gottlieb, H. *Electrochim. Acta* **1989**, *34*, 141.
28. Aurbach, D.; Daroux, M.; Faguy, P.; Yeager, E. *J. Electroanal. Chem.* **1991**, *297*, 225.
29. Aurbach, D.; Zaban, A. *J. Electroanal. Chem.* **1995**, *393*, 43.
30. Piao, T.; Park, S.-M.; Doh, C.-H.; Moon, S.-I. *J. Electrochem. Soc.* **1999**, *146*, 2794.
31. Kim, Y.-O.; Park, S.-M. *J. Electrochem. Soc.* **2001**, *148*, A194.
32. Bockris, J. O'M.; Reddy, A. K. N. *Modern Electrochemistry*; Plenum: New York, 1970; Vol. 2.
33. Sauerbrey, G. *Z. Phys.* **1959**, *155*, 206.
34. Eichinger, G. *J. Electroanal. Chem.* **1976**, *74*, 183.
35. Arakawa, M.; Yamaki, J.-I. *J. Electroanal. Chem.* **1987**, *219*, 273.
36. Aurbach, D.; Daroux, M. L.; Faguy, P. W.; Yeager, E. *J. Electrochem. Soc.* **1987**, *134*, 1611.
37. Ward, M. D. In *Physcial Electrochemistry*; Rubinstein, I., Ed.; Marcel Dekker: New York, 1995.
38. Kang, H.; Kim, K. D.; Kim, K. Y. *J. Am. Chem. Soc.* **1997**, *119*, 12002.
39. Yang, M. C.; Lee, H. W.; Kang, H. *J. Chem. Phys.* **1995**, *103*, 5149.